



**UNIVERSITY
OF TURKU**

This is an Accepted Manuscript version of the article published originally by American Association of Physics Teachers, accepted for publication in the journal:

American Journal of Physics

This version may differ from the original in pagination and typographic details. When using please cite the original.

AUTHOR(S)

Kuusela, T. A.

TITLE

Linewidth measurement of external cavity lasers

YEAR

2024

DOI

10.1119/5.0207084

CITATION

Kuusela, T. A. (2024). Linewidth measurement of external cavity lasers. *American Journal of Physics*, 92(6), 459–465. <https://doi.org/10.1119/5.0207084>

VERSION

Accepted Manuscript

LICENSE

© 2024 American Association of Physics Teachers

Linewidth measurement of external cavity laser

Tom A. Kuusela*

*Department of Physics and Astronomy,
University of Turku, 20014 Turku, Finland*

(Dated: April 19, 2024)

Abstract

Narrowband laser sources are used in applications that require high-precision or stable optical frequency. Such applications include high-resolution spectroscopy, long-distance measurement, and coherent optical communication. The linewidth of a laser is a direct measure of the laser's stability, and therefore characterization of laser linewidth is essential. In practice, however, determining a laser's linewidth is not a trivial task and typically requires expensive equipment or a complex experimental arrangement. This paper presents a straightforward, low-cost method based on unbalanced interferometry, which allows us to determine the visibility of fringe patterns as a function of the optical path difference and, consequently, the linewidth of the laser. As a test laser, we use a tunable external cavity laser source at around 780 nm, where an interference filter is employed for wavelength selection. Data obtained by applying the interferometric technique to this laser and the analysis of these data, along with the resulting linewidth value, are presented. Given that the described measurement setup is inexpensive, straightforward, and pedagogically accessible, it is well-suited for an instructional physics laboratory experiment and will also be of interest to laboratory researchers.

I. INTRODUCTION

Narrowband laser sources are needed in various high-precision measurement setups. Common application areas include fiber-optic and interferometric sensors,¹ spectroscopy, LIDAR,² atomic clocks,³ and high-speed coherent communication systems.⁴ In all of these applications, the linewidth of the laser directly affects the precision of the measurements that can be performed, making its accurate determination an essential task.

The linewidth of a laser is a measure that indicates the full width at half maximum (FWHM) of the optical spectrum of light. Typically, this quantity is expressed in Hertz. The linewidth is closely related to the temporal coherence of the laser light and its characterization in terms of coherence distance or time. The finite linewidth of a CW laser is a consequence of phase noise in the electric field, which can manifest as continuous frequency drift or sudden phase jumps. The most fundamental component of laser noise arises from its quantum mechanical nature, although this is typically very small, and in practice, the noise source is primarily technical, such as environmental acoustic vibrations, temperature fluctuations, and variations in the laser's drive current. Thus, the linewidth directly reflects the stability of the laser source, which is a critical characteristic in all applications.

II. MEASURING LASER LINEWIDTH

The simplest spectrum analyzers are based on a diffraction grating and an array of photodiodes or one-dimensional CCD sensor. A scanning version of a spectrometer is a one- or two-stage monochromator. The resolution of such diffraction-type analyzers is usually quite modest, typically ranging in the tens of GHz at best. In practice, these analyzers are not sufficient for characterizing the linewidth of a laser.

A widely used method for determining narrow linewidth involves mixing the light of the laser under investigation with that of another reference laser with a known linewidth.⁵ When two mutually *incoherent* laser lights, each with a Lorentzian line shape, are mixed, the result is a beat signal whose frequency is the difference between the frequencies of the lasers, and the spectrum also has a Lorentzian shape⁷

$$S(f) = \frac{\Delta f_t + \Delta f_r}{2\pi[(f - f_b)^2 + (\Delta f_t + \Delta f_r)^2/4]}, \quad (1)$$

where Δf_t is the linewidth of the laser under investigation and Δf_r is that of the reference

laser, and f_b is the beat frequency. If the frequency difference between the lasers is small, the beat signal can be directly measured with a fast photodiode, and the current it produces can be analyzed with an electronic spectrum analyzer. If $S(f)$ is measured and Δf_r is known, Δf_t can be calculated from Eq. (1). The method is straightforward but has some serious drawbacks. Firstly, another stable laser is needed, whose frequency is sufficiently close to that of the laser being measured, and its linewidth must be known and must be at most of the same order of magnitude as that being measured. In practice, the linewidth measurement problem simply shifts to characterizing the reference laser. To some extent, these problems can be circumvented by constructing two identical versions of the laser under investigation, whose light is mixed together. If a stabilized reference laser is usable, it is even possible to phase lock another laser into it.⁶

It is also possible to generate a similar beat signal using the laser being measured itself.⁵ In this case, the laser light and its delayed version are mixed together to produce a beat signal (the so-called *delayed self-homodyne interferometric detection*). The delay must be long enough for the light sources to be mutually incoherent, in which case Eq. (1) is valid. If the linewidth is very narrow, the optical path difference required for the delay, essentially an optical cable, must be very long, even several kilometers. With long optical cables, signal attenuation is inevitable, which complicates the method, especially at short wavelengths. A long optical cable is also very susceptible to external interference. Another drawback is the beat signal's center frequency being at zero frequency, making the measurement particularly sensitive to low-frequency environmental disturbances. This problem can be solved by using an acousto-optic modulator in one arm of the mixing, which shifts the frequency of the second source somewhat (*delayed self-heterodyne interferometric detection*). It is also possible to use an optical delay much shorter than the coherence distance, but then determining the linewidth requires complex calculations and assumptions about the shape of the laser's spectra.⁸

Fabry-Pérot interferometers can achieve very high frequency resolution, up to the order of MHz.^{9,10} When the length of the interferometer's cavity is scanned with piezoelectric elements, a tunable narrowband filter is created, which can be used like a spectrum analyzer. However, the use of Fabry-Pérot interferometers is not quite simple. In order for the cavity bandwidth to be narrow, the reflectance of the mirrors used in it must be extremely high (i.e., the finesse of the cavity very high), which is challenging to measure directly.¹¹⁻¹³ It can

be determined by ringing measurements made with a pulsed laser, but this again requires the use of a known laser. In any case, since the output signal's spectrum is the convolution of the cavity mode shape and the laser under investigation's spectrum, the cavity must be well known. The cavity's free spectral range is also limited, and typically, the coating of the required mirrors also only works in a very narrow frequency range. Another problem is feeding the laser light into the cavity in such a way that only the cavity's fundamental mode is excited.

Sometimes it is possible to use the absorption spectrum of a suitable gas to estimate the laser's linewidth. A commonly used example is rubidium gas, which has easily recognizable hyperfine splittings around 780 nm.¹⁴ In practice, a somewhat more accurate estimation of the linewidth requires a Doppler-free saturation approach.¹⁵ In general, this approach has very limited range of useful wavelengths. Determining the laser's linewidth using an absorption spectrum naturally requires that we know the absorption linewidth of the gas used accurately, which usually isn't possible without measurements first made with a known laser. Thus, in this method as well, the problem shifts elsewhere.

An optical spectrum analyzer can also be constructed with a Michelson interferometer, a method known as Fourier transform spectroscopy. By inputting the laser light under investigation into the interferometer, whose arm lengths are varied in a controlled manner, and measuring the output port's intensity as a function of the optical path difference, a so-called interferogram is formed. The Fourier transform of this interferogram yields the laser's frequency distribution. This method is flexible and inherently broadband and does not require other precise information than the magnitude of the optical path difference. In commercial wavemeters, the optical path difference, which is measured with a reference laser, is changed mechanically several times per second across the entire measurement range, but no more than a few tens of centimeters. This corresponds to a frequency resolution of a few GHz. Achieving better frequency resolution would require much longer optical path differences, which are difficult to implement continuously.

In this work, we use the principle of an interferometer to determine the linewidth of a sample laser using significantly longer optical path differences. The interferometric method has several advantages over the other methods presented above. This method is not based on any other well-controlled laser source or gas absorption line, is easily feasible with the same basic structure for very different wavelength ranges, and does not contain any particularly

expensive optical components. With an interferometer, it is possible to achieve a good or even excellent frequency resolution and this approach does not really require any calibration. From a pedagogical point of view, it is easy to build and the principle of operation is simple. In order to test this method, we use a sample laser with a less common external cavity structure, in which the laser's wavelength is adjusted by an interference filter.

III. INTERFEROMETRIC METHOD

We now show how to use the unbalanced Michelson or Mach-Zehnder type of interferometer in linewidth characterization. In this construction, we divide the input laser beam into two beams using a fiber optic 50:50 beam splitter. We assume that both light beams are equally linearly polarized. As the beams are originated from the same source, they have equal spectral distribution. Next, we combine both beams in a second 50:50 non-polarizing beam splitter, after one of the beams has traveled along a longer path than the other beam. The electric output field is then

$$E_{out}(z, t) = E_1(z, t) + E_2(z, t + \tau), \quad (2)$$

where $E_{1,2}$ are the input fields propagating in the z -direction (the direction of the light beam) and τ is the time delay because of the longer optical path of the beam 2. The corresponding averaged output intensity is (we omit the z coordinate)

$$\langle I_{out}(t) \rangle = \langle |E_{out}(t)|^2 \rangle = \langle E_{out}(t)^* E_{out}(t) \rangle = \langle I_1(t) \rangle + \langle I_2(t) \rangle + 2\text{Re}\langle E_1(t)^* E_2(t + \tau) \rangle, \quad (3)$$

where $I_{1,2}$ are the input intensities, the symbol $*$ indicates the complex conjugate, and the brackets $\langle \rangle$ time averaging over a long period

$$\langle f(t) \rangle = \lim_{T \rightarrow \infty} \int_0^T f(t) dt. \quad (4)$$

When $\langle I_1 \rangle = \langle I_2 \rangle = \langle I_{in} \rangle$, we obtain

$$\langle I_{out}(t) \rangle = 2\langle I_{in}(t) \rangle \{1 + \text{Re } g^{(1)}(\tau)\}, \quad (5)$$

where the *degree of the first-order coherence* is (we omit the index of the electric fields)

$$g^{(1)}(\tau) = \frac{\langle E^*(t) E(t + \tau) \rangle}{\langle E^*(t) E(t) \rangle}. \quad (6)$$

We can now utilize the *Wiener-Khinchin theorem*, which states that the coherence $\langle E^*(t)E(t+\tau) \rangle$ and the power spectral density $S(\omega)$ of the light are a Fourier transform pair^{9,16,17}

$$\langle E^*(t)E(t+\tau) \rangle = \mathcal{F}\{S(\omega)\} = \frac{1}{2\pi} \int_{-\infty}^{\infty} S(\omega)e^{-i\omega\tau} d\omega, \quad (7)$$

$$S(\omega) = \mathcal{F}^{-1}\{\langle E^*(t)E(t+\tau) \rangle\} = \int_{-\infty}^{\infty} \langle E^*(t)E(t+\tau) \rangle e^{i\omega\tau} d\tau. \quad (8)$$

We can assume that the spectral density has either a *Gaussian* or *Lorentzian* form. If we have a Gaussian spectrum¹⁶

$$S_G(\omega) = S_0 e^{-\frac{(\omega - \omega_0)^2}{2\sigma^2}}, \quad (9)$$

where ω_0 is the central frequency and σ determines the full width at half maximum $FWHM = 2\sigma\sqrt{2\ln(2)}$ of the spectrum, we obtain

$$\langle I_{out}(t) \rangle = 2\langle I_{in}(t) \rangle \{1 + e^{-\frac{1}{2}(\sigma\tau)^2} \cos(\omega_0\tau)\}. \quad (10)$$

Without the exponential factor in front of the cosine term, Eq. (10) is well-known result for the interference of monochromatic light: the output intensity varies between 0 and $4\langle I_{in}(t) \rangle$ as a function of the delay τ . If we have more realistic spectrum, in general the exponential term represents the *visibility* of the interference. For example, if the delay τ is large, the visibility approaches zero and the interference disappears completely. By measuring the visibility as a function of the delay we can determine the spectral width σ of the laser light. In the case of a Lorentzian spectrum¹⁶

$$S_L(\omega) = S_0 \frac{\gamma/\pi}{\gamma^2 + (\omega - \omega_0)^2}, \quad (11)$$

where 2γ is the *FWHM* of the spectrum, we have similarly

$$\langle I_{out}(t) \rangle = 2\langle I_{in}(t) \rangle \{1 + e^{-\gamma|\tau|} \cos(\omega_0\tau)\}. \quad (12)$$

The original frequency distribution of laser light emitted by the gain medium can indeed be Lorentzian, especially in idealized conditions. The gain medium's natural emission linewidth, also known as the Lorentzian linewidth, characterizes this distribution. The Lorentzian distribution arises from the inherent quantum mechanical properties of the gain medium, where the emission of photons is governed by the energy levels and transition probabilities within the medium. In an idealized scenario with perfect homogeneity and coherence within the gain medium, the emission linewidth would follow a Lorentzian distribution.

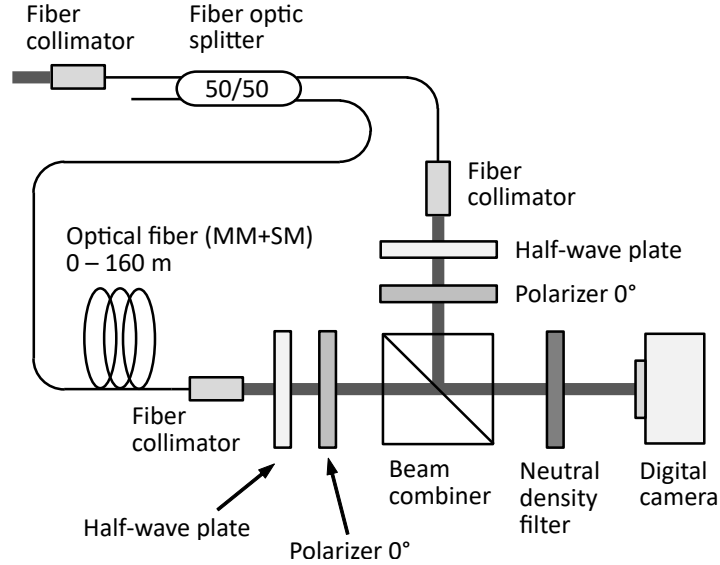


FIG. 1. Interferometer construction.

In practice, however, the frequency distribution of a laser is often Gaussian (or approximately Gaussian) due to several factors. In a laser, amplification of light occurs within a gain medium, such as a gas, liquid, or solid. The gain medium's properties can lead to a Gaussian distribution of photon frequencies. This effect can be due to the distribution of energy levels within the gain medium and the statistical behavior of particles interacting with photons. Thermal effects within the gain medium can cause a broadening of the frequency distribution. As the gain medium heats up, atoms or molecules within it gain kinetic energy, leading to Doppler broadening. In a laser cavity, the resonant modes can influence the frequency distribution of emitted light. These cavity modes often have a Gaussian intensity profile, which can shape the laser's spectral output to be approximately Gaussian. And finally, various noise sources and fluctuations in the laser system, such as electronic noise, mechanical vibrations, or fluctuations in the pump power, can contribute to a Gaussian-like distribution of frequencies in the laser output.

The interferometric linewidth measurement setup is depicted in Fig. 1. Light from the external cavity laser is coupled into the interferometer using a fiber collimator package (Thorlabs F230FC-780) and split into two arms using a fiber optic 50:50 splitter (narrow-band single mode coupler/splitter Thorlabs TN785R5F2). Since a fiber is used to implement the optical path difference, the splitter is fiber optic-based rather than a conventional beam splitter. One arm of the splitter is terminated directly with a collimator, while different

lengths of optical fibers are inserted into the other arm. Finally, this arm is also terminated with a collimator. The beams from both collimators are combined using a 50:50 non-polarizing broadband cube beam combiner (Thorlabs BS011) to generate interference pattern.

The visibility can be determined by slightly varying the delay in Eq. (10) or Eq. (12). In practice, this can be done by changing the distance of another collimator from the beam combiner using a platform that can be moved with micrometer adjustments. If the interferometer is perfectly aligned, i.e., the beams perfectly overlap within the beam combiner, the interference pattern is a dark or bright spot, or something in between, depending on the magnitude of the delay. By measuring the intensity of this spot as a function of delay, we get a series of measurements to which we can match the function given by Eq. (10) or (12) and determine the visibility from it. Since such a series of measurements will inevitably take a considerable amount of time, typically several minutes, the laser being studied must be completely stable for the measurement time period to have meaningful results. As we will show in Sec. V, the frequency of the laser can jump on the timescale of a few seconds, which is why we chose another method of measurement. In this alternate method, the beam splitter is slightly rotated and tilted so that a fringe pattern consisting of a few lines is formed on the camera, from which visibility can be directly determined. Pedagogically, this is also a more beneficial approach, as the student can see directly from the interference pattern how the visibility decreases as the path distance difference increases. In our setup, the interference pattern is projected onto the surface of the camera chip (digital monochrome camera IDS U1-1242L, 1280 x 1024 pixels) and the resulting image is viewed on a computer. A neutral density filter (Thorlabs NE10A) is placed in front of the camera to maximize the camera's dynamic range. The capture time should be kept as short as possible, less than 50 ms.

Since the polarization state of light after the optical fibers is practically unknown, linear polarizers (Thorlabs LPNIRE050-B) are placed in front of both input ports of the splitter at 0° angle (or any other fixed angle). If the polarizations were not exactly the same, it would directly affect the observed visibility. The light after optical fibers is, in general, elliptically polarized, but complete correction for the fiber birefringence is not needed. Half-wave plates (Thorlabs WPH05ME-780) in front of the polarizers are used to adjust the intensities to be exactly the same in both arms. This needs to be done carefully to ensure that the measured visibility reflects only the properties of the laser light. If the light is

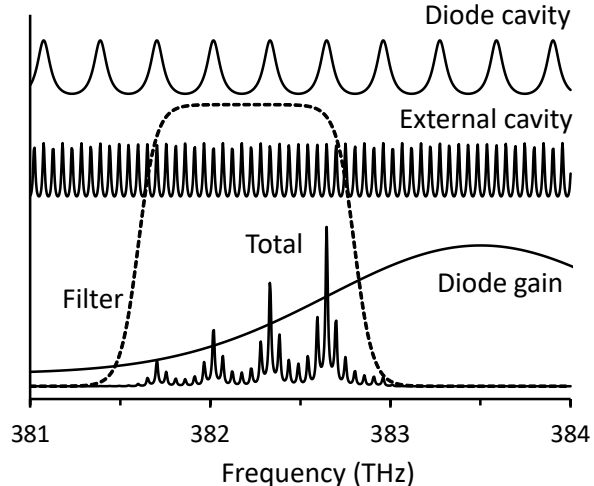


FIG. 2. Frequency-dependent components of the external cavity laser. The total transmission is the product of the transmission of diode cavity and external cavity, the semiconductor gain profile and the transmission of the interference filter.

nearly circularly polarized, an additional quarter-wave plate (Thorlabs WPQ05ME-780) is needed.

The optical path difference is adjusted by adding varying lengths of optical fibers, or combinations thereof, to one arm of the interferometer. To ensure a simple interference pattern, only one spatial mode of light should be used in interference formation. Therefore, theoretically, all fibers should be single mode (SM) fibers.¹⁸ However, long single mode fibers are quite expensive (about \$4/m). In experiments, we found that it is also possible to use multimode (MM) fibers (less than \$1/m), as long as the final segment of the fiber is single mode. The coupling efficiency from multimode fiber to single mode fiber was surprisingly good, about 10–20%. We used 10 m single mode fibers (2 pc, Thorlabs P1-780A-FC-10), 50 m single mode fiber (Thorlabs 780HP), and 100 m multimode fiber (Thorlabs GIF625-100). The longest fibers (50 and 100 m) are terminated with universal bare fiber terminators (Thorlabs BFT1).

IV. LASER SETUP

The most common structure of a tunable external cavity laser follows either the Littrow or Littman–Metcalf configuration, where wavelength selection occurs through a diffraction

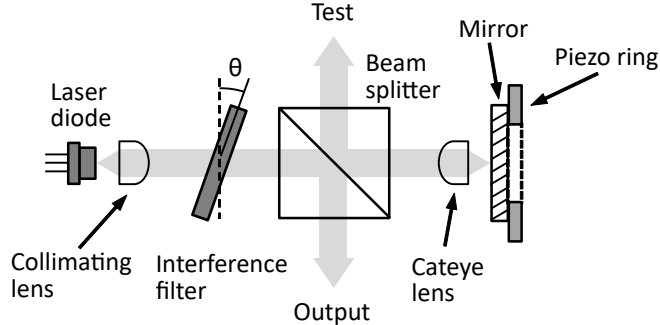


FIG. 3. Setup of the filter tunable external cavity laser.

grating.^{19,20} In the Littrow configuration, the grating acts as the cavity's end mirror. A drawback of this structure is that the direction of the output beam changes as the grating is rotated. In the Littman-Metcalf configuration, the grating orientation is fixed, and an additional mirror is used to reflect the first-order beam back to the laser diode, resulting in a constant direction of the output beam. Both structural types require careful optical alignment and are therefore sensitive to external mechanical disturbances. It is also possible to implement a very simple external cavity laser using just a microscope cover glass as a feedback reflector, but frequency adjustment is then very limited.²¹

A narrowband interference filter provides an alternative way to implement external cavity wavelength selection. Various factors dependent on the frequency of the external cavity laser are presented in Fig. 2.²² The semiconductor chip of the laser diode forms a Fabry-Pérot cavity, typically with a length of $L_d = 0.25$ mm. In this case, the frequency difference between two cavity modes is $c/2nL_d = 125$ GHz, where the refractive index of the semiconductor is $n = 3.5$.⁹ When the laser output signal is reflected back from the end mirror of the external cavity, the laser has the possibility to operate on one or more external cavity modes because the laser gain curve is quite broad Gaussian.

The external longitudinal mode can be selected by a diffraction grating or a filter. The required filter should be very narrow-band, with the emission bandwidth significantly narrower than 1 nm in practice.²³ Such filters are difficult to find in commercial ranges. However, much wider filters can also be used, if their emission bandwidth decreases steeply enough.²⁴ Together with the gain curve, the filter effectively selects one external mode. By rotating the filter, the filter's transmission band can be altered, and the desired external mode can be selected.²⁵ In practice, the laser will oscillate at the frequency for which the product of

all the factors shown in Fig. 2 is greatest.

The setup of the filter tunable external cavity laser is shown in Fig. 2. It consists of a laser diode (Thorlabs L780P010, wavelength 780 nm, and output power 10 mW at a current of 20 mA, no temperature control), an aspheric collimating lens (focal length 4.51 mm), an interference filter (Iridian 785nm BPF, bandwidth 2-3 nm), a cube-type non-polarizing beam splitter (Thorlabs BS011), and finally, a cat's eye reflector (aspheric lens with a focal length of 4.51 mm and a silver mirror glued on a piezo ring Thorlabs P44M3KW). All optical components are assembled using Thorlabs 30 mm optical cage system. Due to the cateye reflector, the mirror's alignment is not highly critical, and therefore, the stability of the cavity and the entire laser to external mechanical disturbances is reduced.²⁶ The length of the external cavity is 50 mm in air and the corresponding mode separation 3 GHz.

The laser wavelength can be adjusted by rotating the interference filter.²⁴ The cavity length can be tuned with a piezoelectric element, enabling fine frequency adjustment. The direction of the laser output beam remains constant, which facilitates the use of the laser. The output power of the laser is about 6 mW, but some of the light also exits from the other side of the beam splitter (Test output, power approximately 3 mW). This output can be utilized, for example, for laser monitoring or locking. Adjusting the laser to operational mode is quite easy without any spectrograph or wavemeter. The laser output power increases sharply when the laser beam is focused precisely on the mirror's surface with the cat's eye reflector lens. In practice, micrometer-level adjustment is necessary.

V. RESULTS

The output spectrum of the laser without an external cavity and with the external cavity and interference filter is shown in Fig. 4. Without an external cavity, the laser has multiple modes. The frequency difference between the modes is about 125 GHz. It is clear that with an external cavity, the laser operates on only one longitudinal mode corresponding to the wavelength of 781.92 nm. However, no conclusions can be drawn about the linewidth of the laser from the latter, as the resolution of the used wavemeter is only about 4 GHz.

When the laser output is coupled to the interferometer and its beam splitter is adjusted appropriately, an interference pattern consisting of a few fringes can be captured by the camera (see Fig. 5 top). From this pattern, an intensity distribution can be further derived

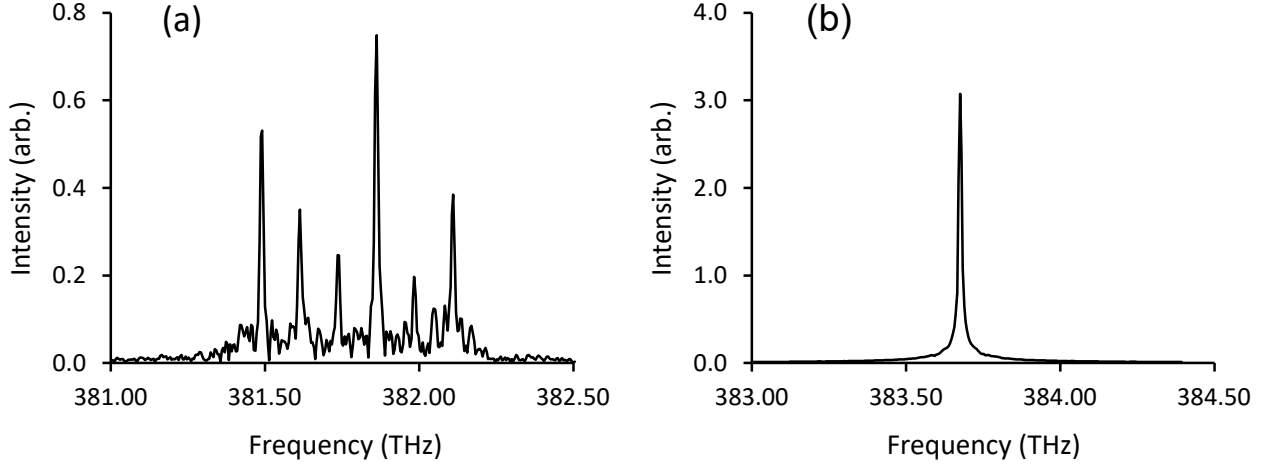


FIG. 4. Spectrum of the diode laser output measured with a wavemeter (a) without any external cavity and (b) with the external cavity. Note the different (but comparable) intensity scale in the figures (a) and (b).

(see Fig. 5 bottom). The interference visibility must be calculated from this distribution. To make the measurement more accurate, a suitable function should be fitted to the pattern. The intensity distribution of a single laser beam after the fiber collimator is Gaussian, and therefore the interference pattern also has a Gaussian envelope. Since the interfering beams travel almost parallel to each other, the interference can be described by a simple cosine function. Thus, the intensity distribution of fringes is modeled with a function

$$I(x) = I_0 \exp\left(\frac{x - x_0}{2\delta}\right)^2 [1 + F \cos(\gamma x)] \quad (13)$$

where x is the pixel number of intensity, I_0 is the intensity of the Gaussian distribution, x_0 its center point, δ the width of the distribution, F the visibility, and γ the spatial frequency of the interference pattern. The measurement is conducted with optical fiber lengths of 0, 20, 60, 110, and 160 m, a single mode fiber of length 10 m is always the last section. As light travels through the optical fiber, the actual optical path difference is the refractive index of the fiber multiplied by the length of the fiber. The refractive index of the fibers is assumed to be 1.45. Ten intensity distributions are recorded for each optical path difference, each fitted according to Eq. (13), and the visibility is determined. The visibility as a function of the optical path difference is shown in Fig. 6. Gaussian [Eq. (10)] and Lorentzian [Eq. (12)] visibility functions are further fitted to the data points using error weighted data values. With Gaussian fitting, the linewidth of the laser was determined to be 0.48 ± 0.02 MHz and

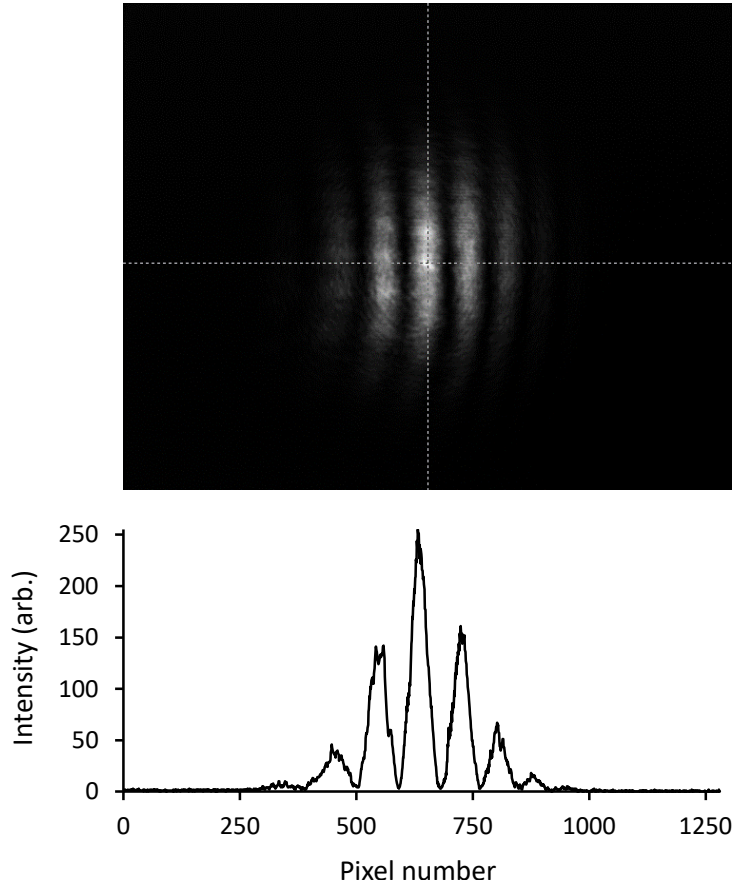


FIG. 5. The interference pattern captured by a digital camera and the corresponding intensity distribution measured along the horizontal dashed line. Pattern is measured with zero optical path difference. The interference pattern has been produced in a situation where the second beam is slightly tilted.

Lorentzian linewidth is 0.15 ± 0.02 MHz. These results can be considered quite good for a laser that is not locked in any way.

Although the statistical deviations of visibility values are moderately large, the mean values follow the Gaussian distribution [Eq. (10)] especially well. This finding may mean that we can provide a reasonably reliable estimate of linewidth, even though we have not measured visibility with very long delays, i.e., we have stopped well before the delayed light beam is completely incoherent with the original one. This feature is a distinct advantage over methods based on Eq. (1), where laser light must be mixed with a clearly incoherent version of itself and much longer optical fibers are needed.

The frequency distribution of the laser should be Lorentzian, but clearly, the experimen-

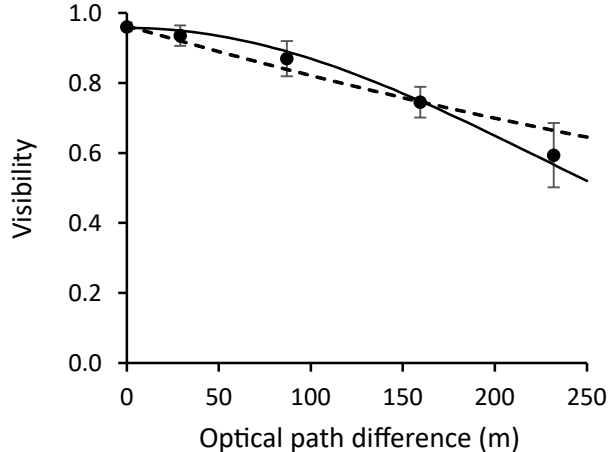


FIG. 6. Visibility of the fringe pattern as a function of the optical path difference. The error bars represent one standard deviation. The solid line represent the numerical fitting of Gaussian visibility and the dashed line Lorentzian one.

tally obtained result does not directly support this assumption. The measured visibility is a combination of the laser’s own internal frequency distribution and all external disturbances. External disturbances, such as mechanical and acoustic vibrations directly affecting the laser, and on the other hand, influences induced by the interferometer and especially its long optical cables, obviously manifest as Gaussian spectra. Since it is difficult to assess the impact of different sources on the measured linewidth, the obtained linewidth can be considered as a pessimistic upper limit for the laser itself.

In addition to measuring linewidth, the interferometer setup can also be used to directly characterize laser stability in time. In experiments, especially with the longest optical path difference, the visibility of the interference pattern do not change much over time, but the entire pattern seen by the live video does occasionally jump. These jumps are obviously due to sudden changes in the laser’s output frequency. According to Eq. (13), a shift of one fringe in the interference pattern corresponds to a frequency change of $\Delta f = 1/(2\tau)$, which for a 160 m optical cable (optical time delay 770 ns) is 0.65 MHz. Larger changes cannot be measured with this measurement system because we do not know how many complete cycles the cosine function has gone through. For stability analysis, the interferometer is adjusted so that the interference pattern consists precisely of one spot, the intensity of which is measured with a photodiode. The spot intensity as a function of time is presented in Fig. 7. Based on this, we can estimate that on the scale of a few seconds, the frequency fluctuates ± 0.1

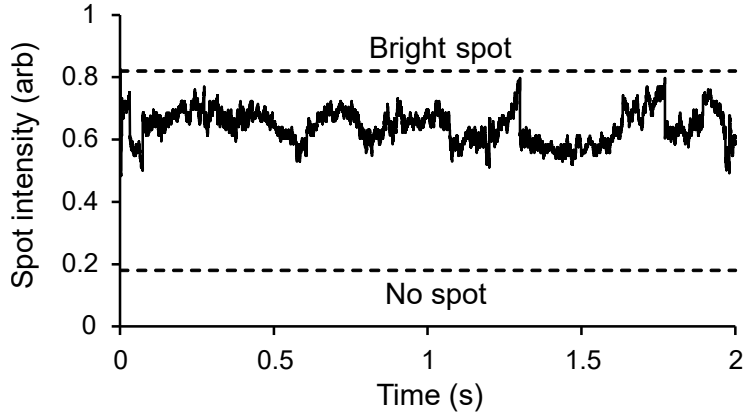


FIG. 7. Intensity of the single interference spot as a function of time when the optical path difference is due to 160 m of optical fiber. The dashed horizontal lines present the intensity level corresponding the brightest and darkest spot. Fluctuations in the intensity reflect changes in the laser frequency.

MHz, but the intensity occasionally jumps abruptly, for which a corresponding frequency change cannot be determined. It is possible that these jumps are related to mode hops of the external cavity. Nevertheless, the result indicates that the laser frequency changes differently on different time scales. Obviously observed frequency jumps partly contribute to statistical deviations of the visibility at long optical path differences.

VI. CONCLUDING REMARKS

The linewidth of the laser is a key parameter in many applications, as it directly reflects the laser's short-term stability. With advancements in technology, linewidths of lasers have already reached the sub-Hz level. Characterizing such laser sources is extremely challenging. However, these lasers offer an unprecedented way to measure very small path differences, for example, for the detection of gravitational waves. Building an external cavity laser in the instructional physics laboratory is not difficult, but measuring the laser's frequency distribution typically requires quite expensive equipment or a complex experimental arrangement, especially when the linewidth is very narrow.

The direct measurement of visibility as a function of the optical path difference presented here provides students with a concrete approach to this topic, as the visibility of the interference pattern is easy to understand and can be observed even with the naked eye. Our

method is versatile and can be easily applied to other wavelength ranges as well. The experimental setup is moderately affordable with the most expensive components being the collimators (\$150 each), beam splitter cubes (\$150) and fiber splitter (\$200). Almost any device can be used as a camera, as the number of pixels or sensitivity is not critical. The cost of optical fibers depends on the linewidth of the laser and therefore the optical distance difference required, but the typical cost is clearly less than \$400. By comparison, a stabilized laser source with a very narrow linewidth that we could use as a reference source costs tens of thousands of dollars.

The measurement method presented here as a teaching tool can also serve as an alternative for research use in determining the linewidth of a laser source. In the delayed self-homodyne/heterodyne interferometric detection method, the optical fiber must be long enough for the mixed beams to be incoherent with each other. With our example laser, it would mean a cable of about 500 m in length, while the approach used here can have a sufficient length of up to 100 m. A shorter cable is a significant advantage, as the attenuation is smaller and the stability of the whole measurement system is better.

* tom.kuusela@utu.fi

¹ T. Zhu, Q. He, X. Xiao, X. Bao, “Modulated pulses based distributed vibration sensing with high frequency response and spatial resolution,” *Opt. Expr.* **21**, 2953–2963 (2013).

² F. Yang, Q. Ye, Z. Q. Pan, D. J. Chen, H. W. Cai, R. H. Qu, Z. M. Yang, and Q. Y. Zhang, “11100-mW linear polarization single-frequency all-fiber seed laser for coherent Doppler lidar application,” *Opt. Commun.* **285**, 149–152 (2012).

³ A. D. Ludlow, M. M. Boyd, and J. Ye, “Optical atomic clocks,” *Rev. Mod. Phys.* **87**, 637–701 (2015).

⁴ K. J. Zhou, Q. L. Zhao, X. Huang, C. S. Yang, C. Li, E. B. Zhou, X. G. Xu, K. K. Y. Wong, H. H. Cheng, and J. L. Gan, “kHz-order linewidth controllable 1550-nm single-frequency fiber laser for coherent optical communication,” *Opt. Expr.* **25**, 19752–19759 (2017).

⁵ Z. Bai, Z. Zhao, Y. Qi, J. Ding, S. Li, X. Yan, Y. Wang, and Z. Lu, “Narrow-linewidth laser linewidth measurement technology,” *Front. In Phys.* **9**, 768165-1–7 (2021).

⁶ F. Friederich, G. Schuricht, A. Deninger, F. Lison, G. Spickermann, P. H. Bolvar, and H. G.

- Roskos, “Phase-locking of the beat signal of two distributed-feedback diode lasers to oscillators working in the MHz to THz range,” *Opt. Expr.* **18**, 8621-8629 (2010).
- ⁷ Z. Fang, H. Chai, G. Chen, and R. Qu, *Single Frequency Semiconductor Lasers* (Springer Nature, Singapore, 2017).
- ⁸ T. Okoshi, K. Kikuchi, and A. Nakayma, “Novel method for high resolution measurement of laser output spectrum,” *Electr. Lett.* **16**, 630-631 (1980).
- ⁹ I. R. Kenyon, *The Light Fantastic: A Modern Introduction to Classical and Quantum Optics* (Oxford University Press, New York, 2011).
- ¹⁰ E. Hecht, *Optics* (Addison Wesley, San Francisco, 2002).
- ¹¹ A. Kyungwon, C. Yang, R. R. Dasari, and M. S. Feld, “Cavity ring-down technique and its application to the measurement of ultraslow velocities”, *Opt. Lett.* **20**, 1068–1070 (1995).
- ¹² J. Poirson, F. Bretenaker, M. Vallet, and A. Le Floch, “Analytical and experimental study of ringing effects in a Fabry-Perot cavity. Application to the measurement of high finesse,” *J. Opt. Soc. Am. B* **14**, 2811–2817 (1997).
- ¹³ J. W. Kim, J. W. Hahn, Y. S. Yoo, J. Y. Lee, H. J. Kong, and H-W. Lee, “Measurement of the linewidth of a continuous-wave laser with a cavity-length modulation technique,” *Appl. Opt.* **38**, 1742–1745 (1999).
- ¹⁴ V. Jacques, B. Hingant, A. Allafort, M. Pigeard, and J. F. Roch, “Nonlinear spectroscopy of rubidium: an undergraduate experiment,” *Eur. J. Phys.* **30**, 921–934 (2009).
- ¹⁵ D. W. Preston, “Doppler-free saturated absorption: Laser spectroscopy,” *Am. J. Phys.* **64**, 1432–1436 (1996).
- ¹⁶ R. Loudon, *The Quantum Theory of Light* (Oxford University Press, New York, 2000).
- ¹⁷ C. Chatfield, *The Analysis of Time Series – An Introduction* (Chapman and Hall, London, 1989).
- ¹⁸ B. E. A. Saleh and M. C. Teich, *Fundamentals of Photonics 2nd Edition* (Wiley, New Jersey, 2007)
- ¹⁹ Y. Cunyun, *Tunable External Cavity Diode Lasers* (World Scientific, Singapore, 2004).
- ²⁰ E. Brekke and T. Bennet, “3D printing an external-cavity diode laser housing,” *Am. J. Phys.* **88**, 1170–1174 (2020).
- ²¹ A. V. Carr, Y. H. Sechrest, and S. R. Waitukaitis, “Cover slip external cavity diode laser,” *Rev. Sci. Instrum.* **78**, 106108-1–3 (2007).

- ²² M. Gilowski, C. Schubert, M. Zaiser, W. Herr, T. Wubbena, T. Wendrich, T. Muller, E. M. Rasel, and W. Ertmer, “Mode stability of external cavity diode lasers,” *Appl. Opt.* **48**, 6692–6700 (2009).
- ²³ D. Saliba, M. Junker, L. D. Turner, and R. E. Scholten, “Narrow bandwidth interference filter-stabilized diode laser systems for the manipulation of neutral atoms,” *Opt. Commun.* **280**, 443–447 (2007).
- ²⁴ D. J. Thompson and R. E. Scholten, “Narrow linewidth tunable external cavity diode laser using wide bandwidth filter,” *Rev. Sci. Instrum.* **83**, 023107-1–5 (2012).
- ²⁵ P. H. Lissberger and W. I. Wilcock, “Properties of all-dielectric interference filters. 2. Filters in parallel beams of light incident obliquely and in convergent beams,” *J. Opt. Soc. Am.* **49**, 126–130 (1959).
- ²⁶ X. Baillard, A. Gauguet, S. Bize, P. Lemonde, P. Laurent, A. Clairon, and P. Rosenbusch, “Interference-filter-stabilized external-cavity diode lasers,” *Opt. Commun.* **266**, 609–613 (2006).